THE GEOLOGY OF AMALTHEA

PHILIP J. STOOKE

Department of Geography, University of Western Ontario, London, Ontario, Canada N6A 5C2

(Received 3 January 1994)

Abstract. Recent developments in image processing, modelling and mapping techniques have been used to produce a revised shape model of Amalthea, a new map of the satellite and improved interpretations of the geology of the satellite. The global shape is influenced by the presence of several very large craters. Several major valleys, probably related to one or more of the largest craters, cross the surface. Bright spots may consist of fresh crater ejecta derived from shallow 'bedrock' at ridges or crater rims rather than recent mass wasting deposits or exposed bedrock.

1. Introduction

The small jovian satellite Amalthea was imaged by Voyagers 1 and 2 (Smith *et al.*, 1979a, 1979b) and described in detail by Veverka *et al.* (1981) who published the first map of the body. Stooke (1992) prepared a shape model and shaded relief map. Improvements in image display and processing software have enabled me to revise the Amalthea shape model and redraw the map, revealing new details and allowing others to be interpreted more reliably.

2. Revision of the Shape Model

The shape model presented by Stooke (1992) was derived from the shapes of limbs and terminators using techniques described in that paper and by Stooke (1986) and Stooke and Keller (1990). It has now been modified as a result of the identification of surface features in areas which had previously appeared nearly featureless. The improvement was made possible by the use of image processing software and hardware which allowed for the display of a larger number of grey levels, rendering hitherto grainy areas with greater clarity and revealing more surface features. Several of the newly-seen features could be identified in at least two images, and showed significant displacement relative to superposed latitude-longitude grids derived from the earlier shape model. This parallax indicates a mis-match between the model and the true shape, most significant between 190° and 270° W within 40° of the equator, where radii in the new model have been reduced by up to 10 km. Although there are still some uncertainties, many features seen in images FDS 16381.29 and 16381.47 can now be correlated with image 16385.31, within the limitations imposed by low resolution (about 4.5 km/pixel) and minor smearing (Figure 1).

Earth, Moon, and Planets **64**: 187–197, 1994.
© 1994 *Kluwer Academic Publishers. Printed in the Netherlands.*

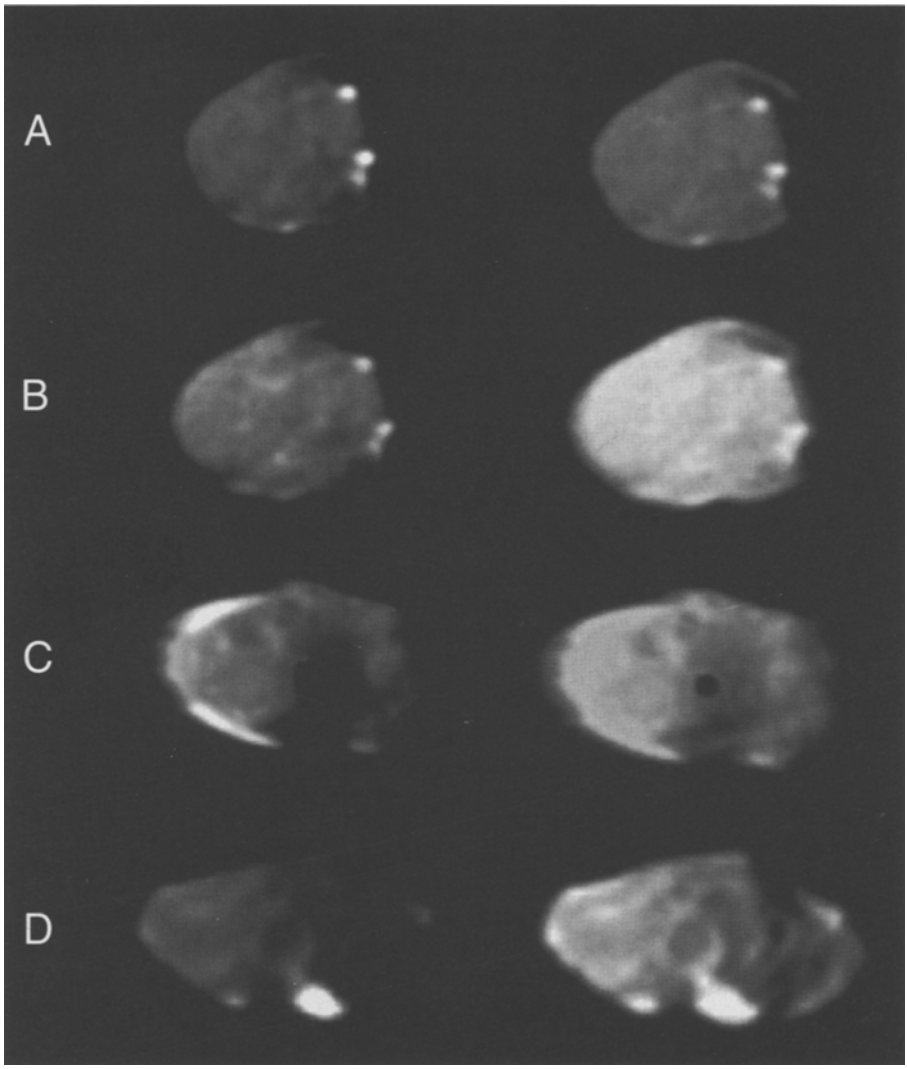

Fig. 1. Images of Amalthea. **A:** FDS 16381.29; **B:** FDS 16381.47; **C:** FDS 16385.31 (the spot is a camera reference mark); **D:** FDS 16377.38. Each image is shown in two versions to emphasize surface features in both bright and dark areas.

3. Results

The surface of Amalthea is illustrated in the form of a shaded relief map (Figure 2) and a topographic map with contours of radii overlain on the relief drawing (Figure 3). The revised topographic data set is presented at 10° spacing in Table I. The full data set at the 5° spacing used for modelling is available from the author on diskette or by electronic mail.

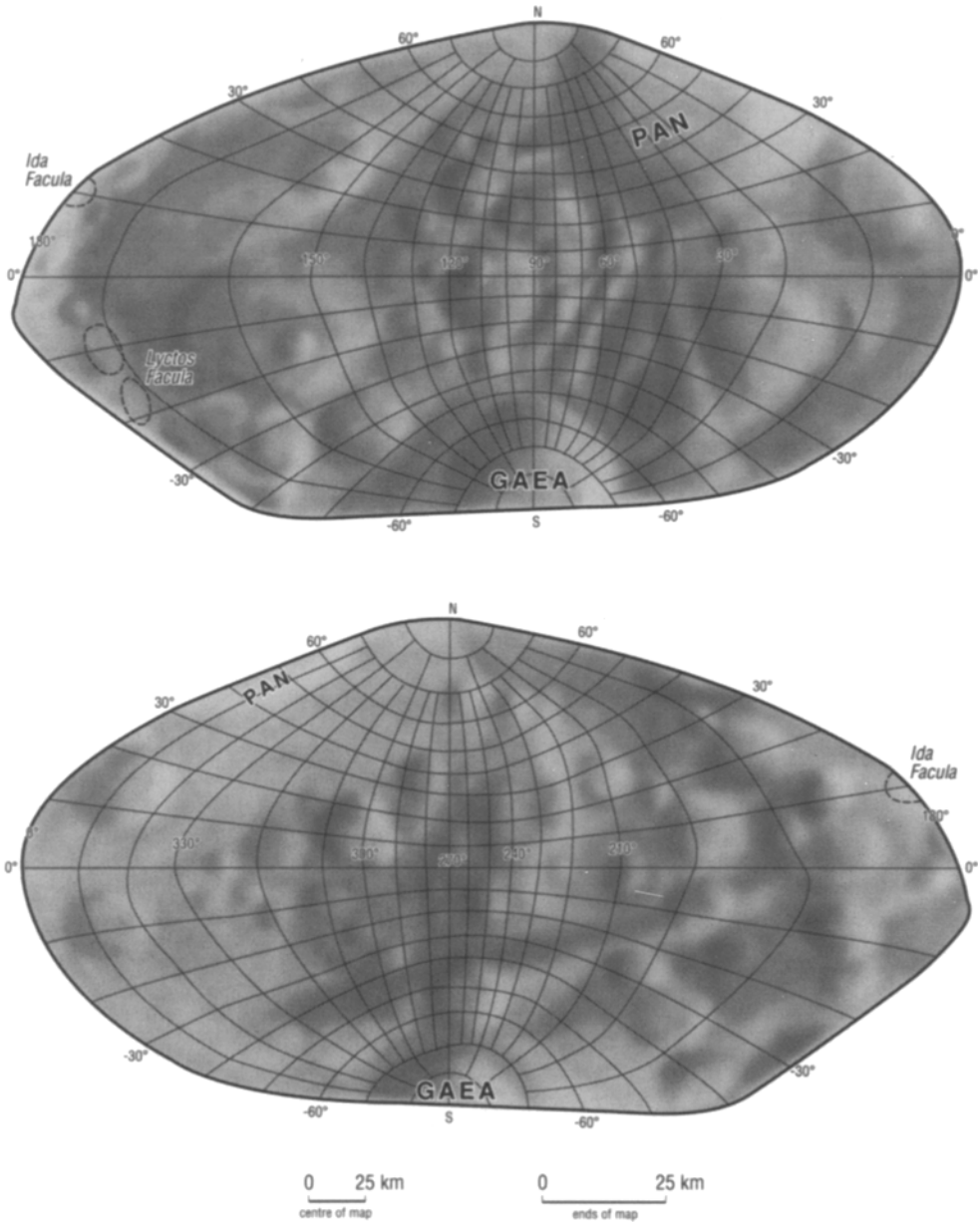

Fig. 2. Shaded relief map of Amalthea on a Morphographic conformal projection derived from the convex hull of the satellite.

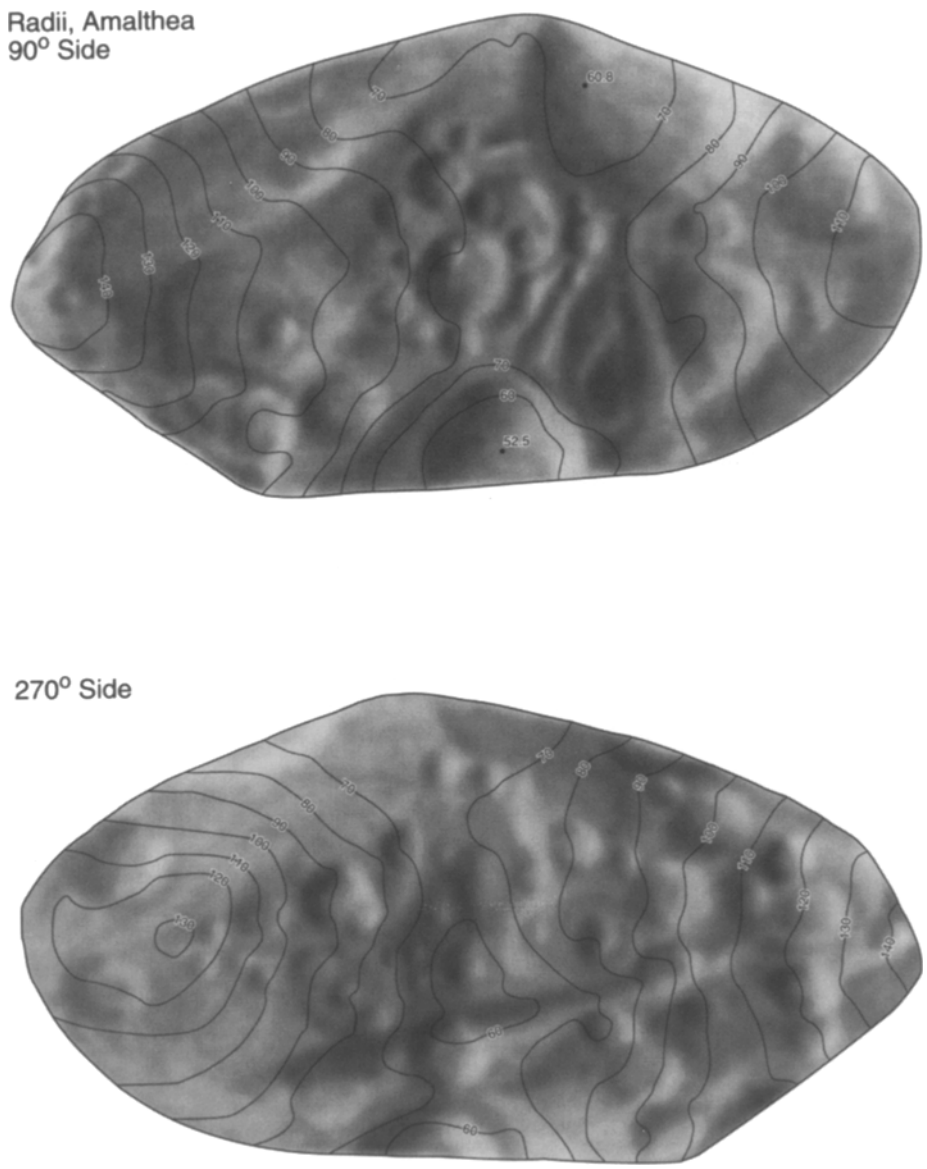

Fig. 3. Shaded relief map of Amalthea with radius contours (radii in kilometres from the assumed centre of mass).

The model is not greatly different from that presented by Stooke (1992) except in the region mentioned above. The maximum and minimum radii are essentially unchanged (150.5 km at 5° S, 175° W and 52.5 km at 80° S, 120° W). The absolute uncertainty in radius estimates is decreased in the region described above, and elsewhere along limb traces of the highest resolution images, to between 5 and

TABLE I

Amalthea: radii (km)

	Longitude									
	90	80	70	60	50	40	30	20	10	0
Latitude										
90	69.5	69.5	69.5	69.5	69.5	69.5	69.5	69.5	69.5	69.5
80	70.2	70.4	70.7	71.0	70.6	70.1	69.7	69.4	69.6	69.7
70	73.0	73.5	73.9	71.9	69.0	66.6	64.5	63.7	64.0	65.0
60	75.0	75.5	74.0	69.7	66.1	63.2	60.8	61.1	63.0	65.2
50	75.5	74.9	72.2	69.3	67.3	64.6	62.9	64.2	66.4	69.9
40	76.5	75.3	72.1	69.0	67.3	67.4	67.1	68.7	72.2	77.3
30	76.5	76.4	74.3	70.9	70.9	71.0	72.2	76.5	81.9	87.2
20	74.0	72.0	72.2	73.3	74.2	74.9	79.0	84.4	94.4	99.6
10	74.0	72.4	71.5	72.7	75.9	82.3	89.8	96.9	105.1	113.2
0	75.3	73.0	72.7	74.7	76.9	83.0	89.9	99.4	110.9	117.8
−10	73.9	72.3	72.7	74.0	76.6	80.0	83.0	92.0	108.1	112.3
−20	73.8	72.4	72.8	73.9	73.0	76.5	80.4	87.8	99.7	104.3
−30	75.0	73.3	73.0	74.4	73.6	73.7	77.5	84.4	92.9	95.8
−40	74.0	73.7	73.0	72.6	70.7	70.6	75.3	81.5	85.8	87.8
−50	69.8	72.4	72.4	72.0	70.6	72.6	76.9	77.6	78.6	80.0
−60	61.0	63.6	68.1	72.8	72.7	72.9	71.4	71.0	72.4	73.7
−70	55.1	56.6	59.1	62.0	62.0	62.8	63.2	63.8	65.4	66.7
−80	53.7	54.0	54.3	54.6	55.5	56.4	57.2	58.1	58.9	59.7
−90	53.0	53.0	53.0	53.0	53.0	53.0	53.0	53.0	53.0	53.0
	Longitude									
	180	170	160	150	140	130	120	110	100	90
Latitude										
90	69.5	69.5	69.5	69.5	69.5	69.5	69.5	69.5	69.5	69.5
80	67.8	67.4	67.6	68.5	69.7	70.1	70.5	70.3	70.2	70.2
70	67.8	67.0	67.3	68.9	71.0	71.2	71.5	71.8	72.3	73.0
60	70.6	67.4	67.7	69.8	73.4	73.4	73.5	73.9	74.5	75.0
50	75.5	70.5	70.1	72.9	76.4	76.2	75.3	74.9	75.4	75.5
40	84.0	76.9	73.9	77.2	80.4	79.2	77.6	76.9	77.1	76.5
30	93.6	88.6	81.3	84.6	85.9	81.0	80.1	78.2	77.3	76.5
20	109.5	105.2	93.9	92.9	92.7	87.9	83.5	78.8	76.0	74.0
10	129.5	130.5	104.5	99.6	98.4	90.0	85.9	80.9	76.8	74.0
0	141.0	139.0	113.0	105.7	99.8	92.9	83.0	77.0	75.0	75.3
−10	138.2	137.5	111.8	101.6	96.7	91.0	77.9	76.2	76.0	73.9
−20	115.0	125.6	108.6	97.6	94.1	88.8	80.6	78.8	76.4	73.8
−30	106.7	104.7	104.0	94.6	91.9	87.3	83.5	79.7	76.6	75.0
−40	102.5	102.4	96.7	91.8	87.1	82.7	79.6	76.3	74.2	74.0
−50	87.0	82.3	79.1	77.1	74.9	73.6	69.9	68.1	68.7	69.8
−60	65.7	62.8	62.1	62.8	62.2	61.8	61.5	60.6	60.5	61.0
−70	57.9	56.3	55.1	54.2	53.9	54.0	54.0	54.0	54.3	55.1
−80	54.6	54.0	53.4	52.8	52.7	52.6	52.5	52.9	53.3	53.7

10 km. Elsewhere it is unchanged, and may be as great as 20 km where no limbs are located (see Stooke (1992) for limb traces on the surface of the satellite). The volume is $2.4 \pm 0.5 \times 10^6$ km^3, about 4% smaller than the value reported by Stooke (1992), but well within the considerable uncertainty of that estimate. If a

TABLE I

Continued

	Longitude									
	270	260	250	240	230	220	210	200	190	180
Latitude										
90	69.5	69.5	69.5	69.5	69.5	69.5	69.5	69.5	69.5	69.5
80	68.5	68.0	67.7	67.6	67.0	66.5	66.6	66.7	67.4	67.8
70	68.7	67.5	66.5	65.9	66.0	65.7	66.0	66.8	67.9	67.8
60	68.8	68.6	68.2	67.6	66.2	66.4	67.4	67.6	69.6	70.6
50	68.9	68.4	68.4	70.3	71.2	71.2	72.0	72.0	74.1	75.5
40	68.8	67.8	67.8	70.9	74.3	76.1	78.9	82.4	84.8	84.0
30	67.9	66.0	67.0	69.1	72.1	76.2	81.0	87.0	94.0	93.6
20	68.5	64.2	65.3	67.5	70.5	73.5	80.8	90.0	98.0	109.5
10	69.1	62.9	62.0	64.0	70.9	74.4	83.2	96.5	108.0	129.5
0	65.8	60.4	58.4	61.5	67.1	72.8	82.6	97.6	117.5	141.0
−10	62.0	58.0	57.6	59.7	62.9	69.1	77.5	87.1	113.0	138.2
−20	61.8	57.8	56.8	58.4	60.0	61.0	70.0	78.0	102.6	115.0
−30	62.8	59.2	56.0	56.0	57.0	62.0	70.0	76.2	93.0	106.7
−40	62.0	59.0	57.0	57.0	60.0	64.0	71.0	77.1	89.0	102.5
−50	64.4	62.0	60.2	62.8	65.9	69.1	74.2	77.8	82.6	87.0
−60	68.1	67.3	66.6	66.0	65.7	65.6	66.8	68.4	66.7	65.7
−70	70.7	69.2	67.7	66.1	64.4	62.7	61.6	60.5	59.3	57.9
−80	60.0	59.5	58.9	58.3	57.6	56.9	56.4	56.0	55.5	54.6
−90	53.0	53.0	53.0	53.0	53.0	53.0	53.0	53.0	53.0	53.0

	Longitude									
	360	350	340	330	320	310	300	290	280	270
Latitude										
90	69.5	69.5	69.5	69.5	69.5	69.5	69.5	69.5	69.5	69.5
80	69.7	69.7	69.6	69.5	69.3	69.2	69.0	68.9	68.8	68.5
70	65.0	65.6	65.8	66.9	67.7	67.7	67.1	67.6	68.4	68.7
60	65.2	68.0	69.2	68.7	69.3	68.9	68.0	67.6	67.9	68.8
50	69.9	72.8	73.3	73.2	73.1	72.3	70.7	69.4	69.1	68.9
40	77.3	81.1	82.2	82.4	80.7	78.0	75.2	72.6	69.6	68.8
30	87.2	91.0	92.8	92.3	89.4	84.7	81.3	77.3	71.0	67.9
20	99.6	102.1	104.5	107.0	103.1	91.2	84.3	83.5	75.8	68.5
10	113.2	115.2	118.1	123.5	111.7	94.0	82.0	82.0	75.7	69.1
0	117.8	122.0	127.0	131.5	113.2	95.9	87.0	79.9	71.3	65.8
−10	112.3	118.0	121.6	120.1	104.4	91.7	82.7	74.5	66.7	62.0
−20	104.3	108.6	109.9	109.3	97.7	78.3	80.7	74.3	66.7	61.8
−30	95.8	100.3	100.0	98.1	91.0	85.4	79.9	77.0	68.1	62.8
−40	87.8	91.1	92.3	87.0	81.5	78.0	74.5	70.9	65.5	62.0
−50	80.0	81.5	80.1	77.4	75.6	72.8	70.9	68.7	66.0	64.4
−60	73.7	73.2	74.8	75.3	74.2	72.9	71.8	70.1	69.0	68.1
−70	66.7	68.6	70.3	70.4	71.0	71.5	72.6	72.1	71.7	70.7
−80	59.7	59.7	59.7	59.6	59.5	59.4	59.6	59.8	59.9	60.0
−90	53.0	53.0	53.0	53.0	53.0	53.0	53.0	53.0	53.0	53.0

triaxial ellipsoid model is required for dynamical calculations, axes of 270, 140 and 122 km give a good match to the overall dimensions and volume. The mass, and thus the bulk density, are unknown.

4. Discussion

The revised map (Figure 2) should be regarded as a 'maximum interpretation'. It shows all craters whose existence can be reliably established, and others (more faintly drawn) which are suspected to exist with varying degrees of certainty, as well as some which appear to be required to explain limb or terminator indentations or subtle shadings on the disk. The drawing style tends to exaggerate the circularity of depressions. Not all are necessarily impact craters. As a result, and also because diameters cannot be measured precisely at the limits of resolution and contrast, no crater statistics are derived here. Nevertheless, impact is the most likely cause of most of these features and the surface is clearly very heavily cratered.

The global shape of Amalthea, apart from its overall elongated form, is dominated by large flattened regions and hollows. Some (e.g. Pan) are clearly craters. Others are more like the roughly flat facets observed on asteroid 951 Gaspra (Thomas *et al.*, 1994) or the south polar saddle on Deimos (Thomas, 1993). For instance, the area between longitudes 180 °W and 280 °W within 40° of the equator is roughly flat or slightly concave, and the south polar region may be slightly saddle-shaped in addition to containing the crater Gaea. In the latter case, Voyager images do not adequately constrain topography near the pole, but as explained by Stooke (1992) Gaea is probably not as large as Veverka *et al.* (1981) suggested and cannot by itself account for all of the south polar depression.

It is likely that all these large features, from obvious impact craters to nearly planar facets, are the results of impact. Thomas (1990) indicates that the south polar saddle of Deimos can be approximately duplicated by forming a large crater on an ellipsoid, and Simonelli *et al.* (1993) show that a few large craters suitably placed on an ellipsoid give a fairly good approximation to satellite shape even if typical crater morphology is not apparent. Recent work by Simonelli *et al.* (1993) and Thomas *et al.* (1994) on shape modelling, and theoretical studies by Greenberg *et al.* (1993) seem to be pointing towards a repudiation of earlier assumptions that impacts on the scale suggested here would catastrophically disrupt a satellite. Craters on small bodies may 'outgrow' the available space during formation and form saddles, flat facets or other non-intuitive shapes. Figure 4 indicates the positions of the largest facets and craters on Amalthea, and the locations of several valleys and bright markings which are described below.

The region between 10° W and 90° W was described by Veverka *et al.* (1981) as containing several parallel ridges and valleys. I previously interpreted some of these structures as nested crater rims (Stooke 1992). A new interpretation is presented here. A single large depression about 70 km across, roughly tangential

to the rims of both craters Pan and Gaea (Figure 1) is centred at 30° S, 30° W. It appears to contain several lesser depressions (later impact craters) which are in turn traversed by a valley extending some 100 km from the rim of Pan (10° N, 45° W) to the terminator near 50° S, 20° W. The valley is about 15 km wide. Its apparent widening to the south in Figure 1 is caused by the enlarged scale near the outer edge of this conformal map projection. A second valley of similar or lesser width runs from 10° N, 60° W to 50° S, 80° W. A third possible valley, short and faint, may extend roughly east-west near 45° N, 90° W. These three valleys are all radial to Pan, the largest well preserved crater on Amalthea (Figure 4a).

Any or all of these might really consist of chance alignments of crater rims, poorly seen at the limited Voyager resolution, but the apparent arrangement radial to Pan lends modest support to their interpretation as fractures. Interpretations of images near the limits of resolution are always uncertain, and greater certainty will not be forthcoming until better images are available.

A long valley, previously described by Stooke (1992), crosses the trailing side of Amalthea from roughly 0° N, 190° W to 50° S, 330° W. When plotted on a conformal projection centred on the south pole (Figure 4), this long valley is seen in relation to the valleys of the leading side, described above. The region around the prime meridian is not seen, so the nature of the connection or intersection of these valleys is unknown. The valleys give the impression that Amalthea has been brought near to fragmentation by a massive impact.

Even on a small low-gravity body like Amalthea, the end of the crater excavation process must be characterized by the deposition of very low velocity ejecta just beyond the rim. The rest of the ejecta may be distributed globally, either directly or re-accreted from Jovian orbit, but the rim should still receive a thicker blanket. Higher resolution images from Galileo may help confirm this for Amalthea, but data for the much smaller satellite Phobos seem to indicate that ejecta is concentrated near the rim of the large crater Stickney (Thomas 1979; Murchie *et al.* 1991). Since at least two valleys extend to the rim of Pan without apparently being masked by late low-velocity ejecta at the rim, they may have been formed or reactivated by the Pan impact.

Several bright markings, or *faculae*, are visible in the Voyager images (Smith *et al.*, 1979a; Veverka *et al.*, 1981). When plotted globally (Figure 4) they appear to occur preferentially on or near the rims of large craters or facets. The significance of this is uncertain, however, given the considerable uncertainties inherent in the shape model, the map itself and the interpretation of individual features. In particular, the diameters of many of the larger inferred facets or depressions are very uncertain, so the positions of rim crests are only approximate. Despite this uncertainty it seems safe to assert that bright markings are concentrated between or on the rims of large depressions rather than in their interiors. As explained by Stooke (1992), the bright marking inside crater Pan is uncertain (and lies on the north outer rim of a small crater on the edge of Pan itself), and the interior of

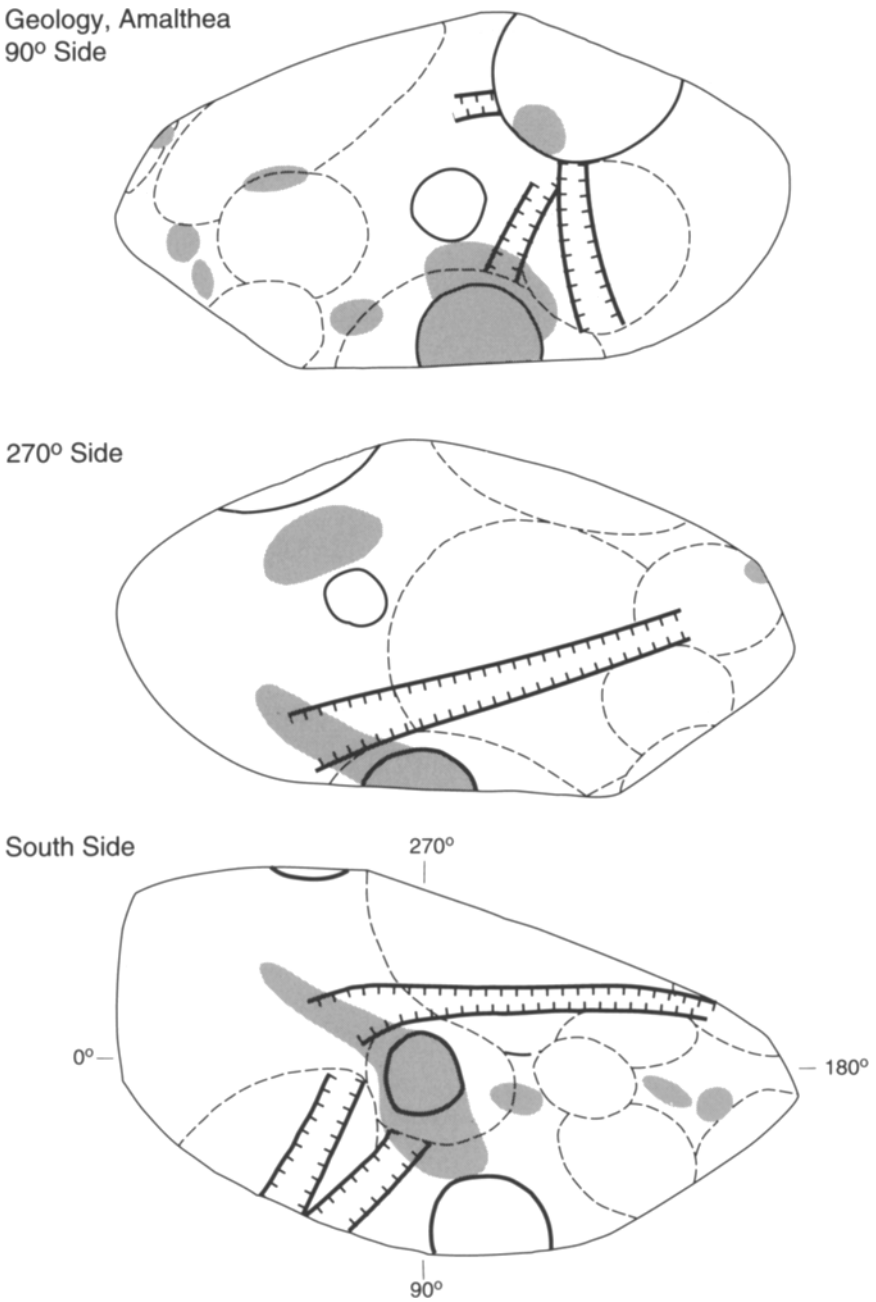

Fig. 4. Sketch maps of surface features of Amalthea on Morphographic conformal projections, viewed from three directions. Dashed loops: degraded, poorly defined or uncertain large craters; solid loops: prominent large craters; heavy double lines: valleys (ticks point down walls); shaded areas: bright markings.

Gaea is poorly seen at best. All other bright spots lie outside or on the rims of the proposed depressions or facets.

Thomas and Veverka (1982) suggested that bright markings were exposures of subsurface material (rock or fresh regolith) exposed by slumping on steep slopes of ridges or crater rims and not yet reddened by sulphur emitted from the volcanoes of Io. More recent work by Thomas (1993) stresses the importance of dynamic topography in questions involving surface transport of debris. Dynamic topography combines physical topography, rotation and tides to find the effective magnitude and direction of slopes on a non-spherical body. The results can vary considerably from physical topography alone. Work currently in progress (P. Thomas, personal communication) on an independent shape model and the dynamic topography of Amalthea will help resolve the question of slopes and the origin of bright markings.

The impression given by Figure 4 is that bright markings are not concentrated on the *inner* walls of the larger craters, despite the likelihood that many sections of them will have steep *local* slopes even if dynamic topography is taken into account. In a few locations small craters appear to be present near bright spots (e.g. Ida and Lyctos Faculae, near longitude 175°.) The largest facula extends as a double lobe outside Gaea at the south pole. These observations suggest that individual faculae may consist of relatively fresh crater ejecta, not yet reddened by exposure to Ionian sulphur.

If 'gardening' by small impacts mixes Ionian sulphur at the surface with lower layers of regolith to produce a deep reddened deposit, bright markings may occur only when an impact excavates material from depths at which contamination by sulphur has not yet occurred. This may occur preferentially near dynamic topography highs (often ridges and large crater rims) which have shed part of their covering of regolith. In the case of Gaea, the crater was sufficiently deep to excavate fresh material despite its formation in a pre-existing depression. This speculation can be tested by obtaining higher resolution imaging during the Galileo mission, timed to place faculae near the terminator for good definition of topography.

5. Conclusion

Galileo images of Amalthea should be sharper than Voyager images of similar geometric resolution. If a wide variety of viewing and illumination conditions can be sampled, the shape model and maps can be improved and the feature interpretations presented here can be clarified. It would be particularly useful to obtain the highest feasible resolution images when prominent bright markings are near the terminator. Global surveys of facula distribution and morphology, and of groove or valley distribution, are needed for this exotic satellite to be better understood.

Since many important features will be only a few pixels across in images of any of the small satellites, care must be taken to ensure that lossy image compression

techniques do not reduce the effective resolution of the images. Transmission of a 100 to 200 line segment of a frame without compression might be more desirable than compression of a full image, if the satellite location within the field of view can be predicted reliably.

Acknowledgements

I thank the National Space Science Data Center and NASA's Planetary Data System, and Bradford A. Smith, Imaging Team leader for the Voyager Project, for making the Voyager data available for this study. I gratefully acknowledge discussions with J. Veverka, P. Thomas and D. Simonelli regarding the mapping of small bodies, and Gordon Shields, David Mercer and Diane Shillington for help with the graphics and manuscript.

References

Greenberg, R., Nolan, M. C., Bottke, W. F., Kolvoord, R. A. and Geissler, P.: 1993, *Bull. Amer. Astron. Soc.* 25 (3): 1138–1139.

Murchie, S. L., Britt, D. T., Head, J. W., Pratt, S. F., Fisher, P. C., Zhukov, B. S., Kuzmin, A. A., Ksanfomality, L. V., Zharkov, A. V., Fanale, F. P., Blaney, D. L., Bell, J. F. and Robinson, M. S.: 1991, *Journal of Geophysical Research* **96**, 5925–5945.

Simonelli, D. P., Thomas, P. C., Carcich, B. T. and Veverka, J.: 1993, *Icarus* **103**, 49–61.

Smith, B. A., Soderblom, L. A., Johnson, T. V., Ingersoll, A. P., Collins, S. A., Shoemaker, E. M., Hunt, G. E., Masursky, H., Carr, M. H., Davies, M. E., Cook, A. F., Boyce, J., Danielson, G. E., Owen, T., Sagan, C., Beebe, R. F., Veverka, J., Strom, R. G., McCauley, J. F., Morrison, D., Briggs, G. A. and Suomi, V. E.: 1979a, *Science* **204**, 951–972.

Smith, B. A., Soderblom, L. A., Beebe, R., Boyce, J., Briggs, G., Carr, M., Collins, S. A., Cook, A. F., Danielson, G. E., Davies, M. E., Hunt, G. E., Ingersoll, A., Johnson, T. V., Masursky, H., McCauley, J., Morrison, D., Owen, T., Sagan, C., Shoemaker, E. M., Strom, R., Suomi, V. E. and Veverka, J.: 1979b. *Science* **206**, 927–950.

Stooke, P. J.: 1986, *Proc. 2nd Internat. Symp. Spatial Data Handling*, Seattle, July 1986, pp. 523–536.

Stooke, P. J.: 1992, *Earth, Moon and Planets* **56**, 123–139.

Stooke, P. J. and Keller, C. P.: 1990, *Cartographica* **27**(2), 82–100.

Thomas, P. C.: 1990, *Reports of Planetary Geology and Geophysics Program – 1989* (Holt, H., ed), NASA Tech. Memo. 4210, Washington, D.C.: National Aeronautics and Space Administration, p. 557.

Thomas, P.C.: 1993, *Icarus* **105**, 326–344.

Thomas, P. C. and Veverka, J.: 1982, Chapter 6 (pp. 147–173) in *Satellites of Jupiter* (Morrison, D., ed). University of Arizona Press, Tucson.

Thomas, P., Veverka, J. and Dermott, S.: 1986, Chapter 17 (pp. 802–835) in J. A. Burns and M. S. Matthews, (eds.). University of Arizona Press, Tucson.

Thomas, P. C., Veverka, J., Simonelli, D., Helfenstein, P., Carcich, B., Belton, M. J. S., Davies, M. E., Chapman, C.: 1994, *Icarus* **107**, 23–36.

Veverka, J., Thomas, P., Davies, M. E. and Morrison, D.: 1981, *Journ. Geophys. Res.* **86**, 8675–8692.